Electromagnetic waves in ferromagnets: a Davey-Stewartson-type model

1999 J. Phys. A: Math. Gen. 32 7907

(http://iopscience.iop.org/0305-4470/32/45/308)

J. Phys. A: Math. Gen. **32** (1999) 7907–7932. Printed in the UK PII: S0305-4470(99)02979-0

Electromagnetic waves in ferromagnets: a Davey–Stewartson-type model

H Leblond

Laboratoire POMA, EP-CNRS 130, Université d'Angers, 2 B^{d} Lavoisier, 49045 Angers, Cedex 01, France

Received 25 March 1999, in final form 11 August 1999

Abstract. We examine the nonlinear modulation of an electromagnetic localized pulse in a saturated bulk ferromagnetic medium. It is seen that the evolution of the pulse shape is governed by a three-dimensional generalization of the Davey–Stewartson (DS) system. A classification of the type of DS system encountered is given, with regard to the value of the physical parameters (external field and wave frequency). Numerical computations show the various possible behaviours of the pulse. Blow-up and spreading out occur, as well as shape modifications. Interaction with electromagnetic long waves can even stabilize the pulse, or cut it into several parts.

1. Introduction

The problem of the propagation of localized multidimensional pulses, or wavepackets, in nonlinear media is presently the subject of intensive research in mathematics, as well as in fundamental or applied physics. The soliton solutions of the one-dimensional nonlinear Schrödinger (1D NLS) equation are well known, but presently their generalization to multiple dimensions is not completely solved. A rather phenomenological point of view considers the so-called two- or three-dimensional NLS (2 or 3D NLS) equation. It gives a quite good account of many experimental results, e.g., the collapse of optical wavepackets in Kerr media. However, it is not integrable in the sense of complete integrability through the inverse scattering transform (IST) method. Therefore, theoreticians studying the IST method consider other generalizations of the 1D NLS equation, that have the integrability property. The most important of these equations is the so-called Davey–Stewartson (DS) system. It was first derived by Davey and Stewartson in the framework of water-wave propagation [1]. It has been shown that it is completely integrable by means of the IST method for particular coefficient values, and admits localized solutions: lumps, algebraically decaying at infinity, and dromions, whose behaviour is very close to that of the 1D solitons, but which are truly 2D [2–6]. The DS system appears to be the correct multidimensional generalization of the 1D NLS equation from this viewpoint, but also from the following one: in every particular physical situation in which it can be relevant, the NLS equation arises as an asymptotic weakly nonlinear behaviour of slowly modulated wavepackets, and is derived using some multiscale expansion, or any equivalent formalism. When performing such an expansion in a rigorous way, starting from some multidimensional model presenting a quadratic nonlinearity, the asymptotic equation obtained is, in most cases, of DS type. It only reduces to the 2D or 3D NLS equation for special situations with a particular symmetry. A recent mathematical theorem by Colin [7] shows that a large class of nonlinear PDEs, able to describe wave propagation in various domains of physics, reduce asymptotically

0305-4470/99/457907+26$30.00

to DS-like systems in such a situation. A recent paper by the present author [8] has shown that the existence of such solitons can be expected for optical pulses in materials presenting a non-vanishing second-order nonlinearity, under some special conditions. On the other hand, the integrable case is rarely reached in concrete physical situations. Numerical and analytical studies of the system show that various behaviours can be expected, showing either collapse or spreading out [9], or less or more stable propagation.

Wave propagation in ferromagnetic media has received new interest for several reasons: on one hand, the so-called Maxwell–Landau model governing these phenomena is of major interest for mathematicians due to its nonlinear properties, and thus also for the theory of nonlinear wave propagation, from the point of view of theoretical physics. On the other, the study of wavepacket propagation in yttrium–iron–garnet (YIG) films has yielded much theoretical and experimental work, which could prove very promising with regard to possible applications [10, 11]. Most of the studies concern the magnetostatic spin waves (MSW) that correspond to the part of the electromagnetic (EM) spectrum where retardation is negligible. The study of MSW has shown the existence of 1D solitons [12, 13] and dark solitons [14]. Interactions of solitons have also been observed [15]. The blow-up of two-dimensional pulses is also known to occur [16].

The present paper, as well as our previous ones [17], deals with the part of the EM spectrum where neither retardation, nor magnetic effects, are negligible. Such waves are often called magnetic polaritons. The propagation of plane waves has been extensively studied, the linear theory was written as early as the 1950s [18–20]. More recently, the weakly nonlinear approximation, and soliton propagation described by the NLS equation have been investigated [17, 21]. Modulational instability involving the excitation of such waves has been observed in a YIG film [22].

The multidimensional generalization of the previous theoretical work is the aim of this paper. After this introductory section, the first step is the derivation of an asymptotic system: the DS system, through a multiscale expansion. This is performed in section 2. The behaviour of the solutions of the DS system depends strongly on the sign of some of its coefficients. Once the asymptotic (DS) system is known, with explicit expressions of its coefficients, a classification can be given. This is done in section 3. Then the asymptotic equations must be solved numerically, as performed in section 4. An important feature is that the numerical scheme used depends on the type of DS system with regard to the above-mentioned classification. When the second equation of the DS system is hyperbolic, boundary conditions are involved, that can be nontrivial. The most important result of this paper is the physical interpretation of these boundary conditions as describing the incident waves in some three-wave interaction, which is resonant in some very particular sense. This interpretation is presented in section 4.2.2 and figure 7. The consequences of the theory from the experimental viewpoint are discussed in section 5, leading to the conclusion. Technical details relating to sections 2 and 3 are given in the appendices.

2. A 3D DS-type system

2.1. Model and ansatz

The propagation of electromagnetic waves is obviously described by the Maxwell equations, with some constitutive relations characterizing the medium in which the wave propagates. In ferromagnetic media, the dependency of the dielectric polarizability with regard to the electric field is linear and scalar, while the magnetic momentum $\vec{M}$ and induction $\vec{B} = \mu_0(\vec{H} + \vec{M})$

are coupled through the so-called Landau equation:

$$\partial_t \vec{M} = -g_L \mu_0 \vec{M} \wedge \vec{B} + \frac{\sigma}{\|\vec{M}\|} \vec{M} \wedge (\vec{M} \wedge \vec{H}) \tag{1}$$

where g_L is the gyromagnetic ratio and σ a negative constant measuring the strength of the damping. Damping is taken into account by the second term on the right-hand side of equation (1), in a phenomenological way. Inhomogeneous exchange interaction, anisotropy and effects related to the finite size of the sample can be taken into account by replacing the magnetic induction $\vec{B}$ in equation (1) by some effective field. We neglect all these effects. This is physically relevant if we study wave propagation, if the wavelength is large enough, if the sample is magnetized to saturation, and if the material is isotropic. After elimination of the electric field, the Maxwell equations reduce to

$$\Delta \vec{H} - \vec{\nabla}(\vec{\nabla} \cdot \vec{H}) = \frac{1}{{c_0}^2} \partial_t^2 (\vec{H} + \vec{M}) \tag{2}$$

where c_0 is the speed of light taking into account the electric permittivity of the medium. Furthermore, the quantities $\vec{M}$, $\vec{H}$ and t are rescaled into $\vec{M}' = \frac{g_L \mu_0}{c_0} \vec{M}$, $\vec{H}' = \frac{g_L \mu_0}{c_0} \vec{H}$ and $t' = c_0 t$, so that the constants g_L, μ_0 and c_0 are replaced by one (in what follows the primes are omitted).

The derivation of the DS-type asymptotic lies on the following multiscale expansion. The fields are expanded in both a Fourier series of some fundamental phase $\varphi = kx - \omega t$, and in a power series of some small parameter ε, as

$$\vec{H} = \sum_{p=0}^{\infty} \sum_{n=-p}^{+p} \varepsilon^p \vec{H}_p^n \mathrm{e}^{\mathrm{i}n\varphi}. \tag{3}$$

Thus ε represents the order of magnitude of the ratio of the wave field amplitude $\vec{H}_1^1$ to the uniform constant field $\vec{H}_0^0$ causing saturation, called the external field. The same expansion holds for the magnetization $\vec{M}$. The amplitudes $\vec{H}_p^n$ are assumed to vary in space and time at a rate which is slow with respect to the wavelength and period of the wave. They depend on slow variables defined by

$$\begin{aligned} \xi &= \varepsilon(x - Vt) \\ \eta &= \varepsilon(y - Wt) \\ \zeta &= \varepsilon(z - Ut) \\ \tau &= \varepsilon^2 t. \end{aligned} \tag{4}$$

The slow 'space' variable $\vec{\xi} = (\xi, \eta, \zeta)$ describes the shape of the pulse propagating at the speed $\vec{V} = (V, W, U)$, while the 'time' variable τ accounts for the evolution of this shape during this propagation. The speed $\vec{V}$ is to be determined: it is in fact the group velocity of the wave. It is easily checked by considering the dispersion relation that this group velocity is not parallel to the phase velocity (chosen as the x-axis), unless the external field $\vec{H}_0^0$ is parallel to the propagation direction. This will be assumed below and it will be shown that W and U are zero in the case considered. Recall that the variable ξ describing the longitudinal shape of the pulse could also be written as a time variable, while the propagation could be written in terms of a distance. The difference between the two variables lies in their order of magnitude only: the order ε corresponds to lengths of the order of λ/ε, assumed to be the size of the pulse, while the propagation variable τ of order ε^2 corresponds to propagation distances with an order of magnitude λ/ε^2 (λ is the wavelength of the fundamental). The expressions for the quantities involved simplify in the particular case considered here, as was already noticed when studying the analogous 1D problem. Therefore, the computation of the successive terms of the

perturbative scheme can only be explicitly achieved in this special case, and the corresponding assumption will be used below.

On the other hand, the study of soliton-like propagation, and other behaviours involving both long-distance propagation and nonlinearity makes no sense if damping is not negligible, or at least can be considered as a higher-order perturbation. Indeed, the possibility of wave propagation implies that the damping is weak: the absorption length must be large with respect to the wavelength. In the same way, the modulational instability occurs only if the absorption length is long enough, so that the instability occurs before the wave is absorbed. However, the rate at which the modulational instability develops can be increased by increasing power input and decreasing the pulse size, in such a way that it occurs faster than damping; but the damping constant σ must be small by itself. By chance this condition is satisfied in the ferrites. The dimensionless quantity

$$\tilde{\sigma} = \frac{\sigma}{\mu_0 g_L} \tag{5}$$

always has a low value: for single-crystal ferrites, $0.01 < \tilde{\sigma} < 0.1$, and, for YIG films, $\tilde{\sigma}$ can reduce to a value of just below 10^{-4}, for a resonance full linewidth $\Delta H \simeq 0.6$ Oe [23]. It thus can be treated in a perturbative way, as in [24]. We assume that

$$\tilde{\sigma} = \varepsilon^2 \hat{\sigma} \tag{6}$$

$\hat{\sigma}$ having an order of magnitude of one. For YIG, considering the above value of $\tilde{\sigma}$, the perturbative parameter ε must be about $\varepsilon \simeq 10^{-2}$. For a larger power input and a shorter pulse length and width, larger values of ε can be envisaged, so that $\tilde{\sigma}$ becomes of order ε^3, and the parameter $\hat{\sigma}$ defined by (6) can be taken as zero. The validity of this approximation is discussed in detail, from the theoretical viewpoint, in [24], and experimentally confirmed in [12].

2.2. Resolution of the perturbative scheme

Expansion (4) is reported into the basic equations (2) and (1), and the perturbative scheme is then solved order by order. At order ε^0 it is found that the saturation magnetization $\vec{M}_0^0$ is parallel to the external field $\vec{H}_0^0$. No demagnetizing factors are taken into account here: $\vec{H}_0^0$ is the field created in the medium by some applied constant and uniform field $\vec{H}_{0\text{ext}}$, but with $\vec{H}_0^0 \neq \vec{H}_{0\text{ext}}$. According to the above assumption, we set

$$\vec{M}_0^0 = \vec{m} = \begin{pmatrix} m \\ 0 \\ 0 \end{pmatrix} \tag{7}$$

and consequently the zero-order condition can be expressed as $\vec{H}_0^0 = \alpha \vec{m}$. The α parameter represents the strength of the external field.

As usual, order ε yields the dispersion relation, and the definition of the possible polarizations:

$$\begin{aligned} \vec{H}_1^1 &= \begin{pmatrix} 0 \\ \mathrm{i}\delta \\ 1 \end{pmatrix} g \\ \vec{M}_1^1 &= -\gamma \begin{pmatrix} 0 \\ \mathrm{i}\delta \\ 1 \end{pmatrix} g \end{aligned} \tag{8}$$

where g is a function of the slow variables $(\vec{\xi}, \tau)$ to be determined and the parameter $\delta = \pm 1$ specifies the circular polarization. The other parameter $\gamma = -1/(\alpha + \delta\nu)$, where $\nu = \omega/m$ is a normalized frequency parameter. The dispersion relation can be expressed as

$$\omega = k\sqrt{\frac{\alpha + \delta\nu}{\alpha + \delta\nu + 1}}. \tag{9}$$

At second order, the equations regarding the fundamental frequency ($n = 1$) yield, as a compatibility condition, the value of the velocity V (equation (46) in appendix A). In particular, it is proved that the group velocity $\vec{V}$ is collinear to the phase velocity: $W = U = 0$. Technical detail is given in appendix A. The important feature is that the equations for the zero-harmonic or mean-value terms $\vec{H}_2^0$ or $\vec{M}_2^0$, coming from (1), are trivial at this order. The corresponding conditions are found at order ε^4. Together with the conditions yielded by the Landau equation at order ε^2 and ε^3 (the compatibility condition in the latter case), they allow one to express $\vec{H}_2^0$ and $\vec{M}_2^0$ in terms of some auxiliary fields Φ, Φ', Φ'', as

$$\vec{H}_2^0 = \begin{pmatrix} \Phi + \frac{2\gamma^2}{m}(|g|^2 - \rho^2) \\ \frac{\alpha}{1+\alpha\beta}\Phi' \\ \frac{\alpha}{1+\alpha\beta}\Phi'' \end{pmatrix} \qquad \vec{M}_2^0 = \begin{pmatrix} \frac{-2\gamma^2}{m}(|g|^2 - \rho^2) \\ \frac{1}{1+\alpha\beta}\Phi' \\ \frac{1}{1+\alpha\beta}\Phi'' \end{pmatrix} \tag{10}$$

where ρ^2 is some limit of $|g|^2$.

The equation obtained at order ε^3 for the fundamental frequency yields, as a compatibility condition, the evolution equation for the amplitude g. It reads

$$\mathrm{i}A\partial_\tau g + B\partial_\xi^2 g + C(\partial_\eta^2 + \partial_\zeta^2)g + D(|g|^2 - \rho^2)g + Eg\Phi + \mathrm{i}\Sigma g = 0. \tag{11}$$

The computational detail is given in appendix A. The equation governing the evolution of the auxiliary field Φ results from the way it was defined when it was introduced in order to solve the Maxwell equations at order ε^4 for the mean-value field. This equation reads

$$\partial_\xi^2\Phi - F(\partial_\eta^2 + \partial_\zeta^2)\Phi = G(\partial_\eta^2 + \partial_\zeta^2)(|g|^2 - \rho^2). \tag{12}$$

The explicit value of the coefficients of equations (11), (12) is of major interest for our purpose. Their expressions have been computed in terms of the α parameters, representing the external field strength, ν, normalized frequency, and $\delta = \pm 1$, characterizing the polarization. They are given in appendix A.

3. Classification of the DS systems

3.1. A word about damping

The last term in equation (11) accounts for the damping. We shall neglect it completely thereafter. More precisely, we set $\hat{\sigma} = 0$. This means that the pulse amplitude is large enough, and its length long enough, so that $\tilde{\sigma}$ has the order of magnitude of ε^3, instead of ε^2, as was assumed above. This simplification is also allowed for the following reasons: the damping only appears in the system (11), (12) through the term $\mathrm{i}\Sigma g$ in the first equation. A very important feature is that the effect of damping on the auxiliary field Φ is completely negligible for the considered scaling. In other words, if the damping does not completely dominate the nonlinear self-modulation of the fast-oscillating wave described by g, the long waves described by Φ are not absorbed in a significant way (see section 4.2.2 for details concerning the physical interpretation of $\Phi \propto \psi$).

The effect of the damping term $\mathrm{i}\Sigma g$ in equation (11) can be largely determined from simple qualitative considerations. Neglecting all terms except this one, equation (11) is reduced to

$\partial_\tau g = \frac{-1}{\tau_0} g$, whose solution is $g = g_0 \mathrm{e}^{\frac{-\mathrm{i}\tau}{\tau_0}} = g_0 \mathrm{e}^{\frac{-\mathrm{i}t}{T_0}}$, where $T_0 = \frac{\tau_0}{c_0 \varepsilon^2}$. T_0 is thus the absorption time, given by

$$T_0 = \frac{2(\alpha + \delta\nu)(\alpha + \delta\nu + 1) - \delta\nu}{-c_0 \tilde{\sigma} m \nu^2}. \tag{13}$$

This expression coincides with the results of [24]. Further, most of the effects described by the numerical computations below occur very quickly (in the examples presented in the various figures, the dimensionless time variable T varies from 0.05 to 0.4). Therefore, it can be reasonably assumed that the effect of a nonzero but quite small damping term is not qualitatively appreciable after such a small propagation time. For all these reasons, the solutions neglecting absorption can reasonably describe the real situation (with damping). It must be kept in mind that the approximation is only valid if the pulse is small enough, the power input large enough, and if the propagation time is not too lengthy.

On the other hand, the solutions of the DS system have the advantage of a great generality, and of being the matter of important mathematical research with many results of physical interest. Therefore, we restrict ourselves to the case where the model is the DS system. In the various restrictions for the system (11), (12) listed below, we make the same assumption $\hat{\sigma} = 0$, for consistency. It is very easy to take the damping into account in these equations, by simply keeping the term $\mathrm{i}\Sigma g$ instead of dropping it.

3.2. Reductions to the NLS equation

Equation (12) is trivially integrated for any 1D reduction, that is, from the mathematical point of view, when looking for solutions depending only on τ and a single space variable $\hat{\xi} = a\xi + b\eta + c\zeta$ (a, b and c being real constants). The so-called 'temporal' case $\hat{\xi} = \xi$ corresponds to propagation in a 1D waveguide, while the so-called 'spatial' case $a = 0$ corresponds to a continuous wave propagating in a plane guide. In these particular cases the evolution equation (11) always reduces to the NLS equation, but with different values of the nonlinear constant.

Assuming that Φ vanishes as $\hat{\xi} \to -\infty$, it can be expressed as

$$\mathrm{i}A\partial_\tau g + B'\partial_{\hat{\xi}}^2 g + D' g(|g|^2 - \rho^2) = 0 \tag{14}$$

where the constants B' and D' read as follows:

- Temporal case.
  The assumption is $\hat{\xi} = \xi$. Then
  $$B' = B \qquad \text{and} \qquad D' = D. \tag{15}$$
- Spatial case.
  We assume that $a = 0$, and normalize b and c so that $b^2 + c^2 = 1$. Then
  $$B' = C \qquad \text{and} \qquad D' = D - \frac{EG}{F}. \tag{16}$$
- Spatiotemporal case.
  This is the general case. We set $a = \cos\theta$ and $b^2 + c^2 = \sin\theta$. The two special cases above are found again by setting $\theta = 0$ or $\pi/2$. Here we have
  $$B' = B\cos^2\theta + C\sin^2\theta \qquad \text{and} \qquad D' = D + \frac{EG\sin^2\theta}{\cos^2\theta - F\sin^2\theta}. \tag{17}$$

Another case where equation (12) integrates is the 2D reduction where the fields do not depend on ξ, that is, where the wave is not modulated longitudinally. That is the situation called 'spatial', describing the variations during propagation of some continuous wave. In this case the evolution equation (12) reduces to the so-called 2D NLS equation:

$$\mathrm{i}A\partial_\tau g + B'(\partial_\eta^2 + \partial_\zeta^2)g + D'g(|g|^2 - \rho^2) = 0 \tag{18}$$

where the constants B' and D' have the same value as in the spatial 1D case given above (equation (16)).

Other 2D reductions of the system (11), (12) are obtained by assuming that g and Φ do not depend e.g. on η, and describe the evolution of a wave that is not modulated in the y-direction, e.g., because it propagates in some planar waveguide. In any of these reductions, the second equation is not trivial, and the system has the same form as the so-called DS system.

3.3. The integrable DS equation

In order to check the integrability of its 2D reduction to the DS system, the model derived in the previous section is reduced to

$$\mathrm{i}\partial_T\phi + \partial_X^2\phi + \epsilon_1(\partial_Y^2 + \partial_Z^2)\phi + \epsilon_2\phi(|\phi|^2 - \sigma^2) + r\phi\psi = 0 \tag{19}$$

$$q\partial_X^2\psi + (\partial_Y^2 + \partial_Z^2)\psi = (\partial_Y^2 + \partial_Z^2)(|\phi|^2 - \sigma^2) \tag{20}$$

through the transform

$$\begin{aligned} X &= \xi \\ Y &= \sqrt{\left|\frac{B}{C}\right|}\eta \\ Z &= \sqrt{\left|\frac{B}{C}\right|}\zeta \\ T &= \frac{B}{A}\tau \\ \psi &= \frac{-F}{G}\sqrt{\left|\frac{D}{B}\right|}\Phi \\ \phi &= \sqrt{\left|\frac{D}{B}\right|}g \\ \sigma^2 &= \left|\frac{D}{B}\right|\rho^2 \end{aligned} \tag{21}$$

where $\epsilon_1 = \pm 1$, $\epsilon_2 = \pm 1$ and r and q are real constants. They read

$$\begin{aligned} \epsilon_1 &= \mathrm{sgn}\,(BC) \\ \epsilon_2 &= \mathrm{sgn}\,(BD) \\ r &= -\epsilon_2\frac{EG}{FD} \\ q &= -\epsilon_1\frac{C}{FB}. \end{aligned} \tag{22}$$

The so-called 2D spatio-temporal reduction of system (19), (20) is obtained under the assumption that the fields ϕ and ψ do not depend on the variable Z. More generally, a single transversal space variable $\hat{Y} = Y\cos\theta + Z\sin\theta$ should be considered, but all values of θ are equivalent because of rotational symmetry around the propagation direction (X-axis). We

assume further that g ($\propto \phi$) vanishes at infinity, so that $\sigma^2 = 0$. As mentioned in the previous section, system (19), (20) reduces to the DS system, which reads as follows:

$$\mathrm{i}\partial_T \phi + \partial_X^2 \phi + \epsilon_1 \partial_Y^2 \phi + \epsilon_2 \phi |\phi|^2 + r\phi\psi = 0 \tag{23}$$

$$q\partial_X^2 \psi + \partial_Y^2 \psi = \partial_Y^2 |\phi|^2. \tag{24}$$

It is thus clear that system (19), (20) is a 3D generalization of the DS system. The DS system (23), (24) is completely integrable by means of the IST method when the two following conditions are satisfied:

$$\epsilon_1 q = \epsilon_2 r + 1 \tag{25}$$

$$\epsilon_1 q = -1. \tag{26}$$

Condition (25) obviously reduces to $\epsilon_2 r = -2$ when (26) is satisfied, but by itself it is sufficient to ensure the existence of the bilinear Hirota form of the system. When integrable, the DS system admits an N-soliton solution, but the involved solitons are quasi-1D. Lump solutions, algebraically decaying in all directions, exist when $\epsilon_1\epsilon_2 = -1$. Solitons exponentially decaying in all directions, called dromions, exist when $\epsilon_1 = 1$. Dromions involve nonvanishing asymptotic conditions at infinity for the auxiliary field ψ, that is, the zero-frequency amplitude Φ. There are, in fact, four integrable systems, depending on the signs ϵ_1 and ϵ_2. The integrable case with $\epsilon_1 = +1$ is called DS I for both values of ϵ_2. When $\epsilon_1 = -1$, it is called DS II. In the general case, system (23), (24) with arbitrary coefficients is not integrable. In [25] it is called the Djordjevic–Redekopp system, while the name DS (DS I and DS II) is kept to the integrable case only. We shall use the terminology of [26], and denote even the non-integrable case by DS.

The integrability conditions (25) and (26) can be solved explicitly in the present case. They yield $\epsilon_2 r = -2$, that reduces, using the expressions (25) and (71)–(74) of the coefficients, to $\Omega (= \alpha + \delta\nu) = -\frac{1}{2}$. The simplification of the result is due mainly to the fact that the complicated coefficients F and G appear in r only through their ratio, that has a very simple expression. But when this condition is satisfied, the coefficient C (its expression is (70)) vanishes, and so does the reduced coefficient q. Therefore, condition (26) cannot be satisfied: the system is never integrable by means of the IST method. $C = 0$ means the vanishing of the transverse derivative in equation (11) for the oscillating wave, while $q = 0$ means the vanishing of the longitudinal derivative in equation (20) for the rectified field. The non-equivalence between $q = 0$ and $C = 0$ is explained by the fact that some coefficients in transform (21) are not finite when $C = 0$. When $q = 0$, the latter equation (20) is trivially integrated, and the system reduces to a 2D NLS equation. As $C = 0$, the first equation (11) of the system reduces to a 1D NLS equation, apart from the term involving Φ. Thus our attempt to obtain a completely integrable system forces it to become closer to the 1D NLS equation. This is related to the fact that the only completely integrable situation is when the system reduces to the 1D NLS equation. Complete integrability is not a purely mathematical property, but is related to the existence of an infinite number of conserved densities. Through the above-mentioned features, it is apparent that such conservation laws cannot be satisfied in ferromagnets except for 1D situations.

The condition necessary for the existence of a bilinear Hirota form for the DS system (23), (24) is (25), without (26). It can be reduced to some algebraic equation involving α and Ω: $\alpha^2(1 + 3\Omega + 8\Omega^2 + 8\Omega^3) + \alpha\Omega(3 + 19\Omega + 28\Omega^2 + 8\Omega^3) + 2\Omega^2(2 + 9\Omega + 10\Omega^2 + 4\Omega^3) = 0$. This equation has no positive real solution when $\Omega \in (\mathbb{R} \setminus [-1, 0])$, which is its allowed range. Thus the bilinear Hirota form also never exists in ferromagnets, except for 1D problems.

Table 1. The various types of DS systems.

$(\epsilon_1, \text{sgn}\,(q))$	Type
$(1, 1)$	elliptic–elliptic
$(1, -1)$	elliptic–hyperbolic
$(-1, 1)$	hyperbolic–elliptic
$(-1, -1)$	hyperbolic–hyperbolic

3.4. A classification

The non-integrable situation, when at least one of the conditions (25) and (26) is not satisfied, is also classified according to the value of ϵ_1 and the sign of the q coefficient, as table 1 shows. Despite the fact that the properties may differ according to the dimensionality, the same classification is also clearly relevant for the 3D generalization (19), (20).

A canonical form has been given in [25], for the system (23), (24) and more general 2D systems of cubic NLS type. It reads

$$\mathrm{i}\partial_T Q + \mathcal{O}_1 Q = P Q \tag{27}$$

$$\mathcal{O}_2 P = \mathcal{O}_3 Q^* Q \tag{28}$$

where $\mathcal{O}_1$, $\mathcal{O}_2$, and $\mathcal{O}_3$ are second-order linear differential operators. In the present case,

$$\left.\begin{array}{l} \mathcal{O}_1 = \partial_X^2 + \epsilon_1 \partial_Y^2 \\ \mathcal{O}_2 = q\,\partial_X^2 + \partial_Y^2 \\ \mathcal{O}_3 = -\epsilon_2 \mathcal{O}_2 - r\,\partial_Y^2 \end{array}\right\} \quad \begin{array}{l} P = -r\psi - \epsilon_2 |\phi|^2 \\ Q = \phi \end{array} \tag{29}$$

thus ϵ_1 and q are either positive or negative when $\mathcal{O}_1$ and $\mathcal{O}_2$ are either elliptic or hyperbolic, respectively.

The relative sign of the dispersion–diffraction term and the cubic nonlinear term is *a priori* also important. It is related to the signature of $\mathcal{O}_3$ in the theory of [25]. But the distinction between the incident oscillating pulse described by ϕ and the long waves described by ψ is of major interest for our purpose, while it is hidden by the canonical form. Therefore, we have left this latter presentation to one side. Recall that, in the case of the 1D NLS equation (14), modulational instability occurs when the $B'D'$ product is positive, and an incident plane wave is destroyed, bunching into solitons (Benjamin–Feir instability). When $B'D' < 0$, plane waves are stable, and only dark-soliton solutions exist. The former case is referred to as focusing, the latter as defocusing. It has been shown (see, e.g., [27]) that collapse or blow-up of the solution of the 2D NLS equation (18) may occur when $B'D' > 0$, while in the case where $B'D' < 0$ the solution always exists globally. An analogous feature has also been proved in the 3D case.

With respect to the 2D DS system, or the 3D version (19), (20), an analogous feature is expected, at least when the first equation (23), or (19) are elliptic. Thus the case $\epsilon_2 = +1$ will be referred to as focusing, and $\epsilon_2 = -1$ as defocusing. The classification rests on an elementary mathematical analysis of the coefficients, that is detailed in appendix B, and the result is summarized in figure 1, on a plot of the dispersion relation. The three branches are labelled N, PA , PO, for negative helicity, acoustic with positive helicity and optical with positive helicity, respectively. It is seen that most sign cases occur. The elliptic–elliptic defocusing case, and the hyperbolic–hyperbolic case are not reached.

A regimen transition occurs on the PO branch, for the normalized frequency $\nu = \nu_0$ defined by expression (81) in appendix B. The following asymptotic expression can be given for ν_0:

$$\nu_0 = 2\alpha + \frac{1}{2} + \frac{1}{8\alpha} + \mathrm{O}\left(\frac{1}{\alpha^2}\right) \tag{30}$$

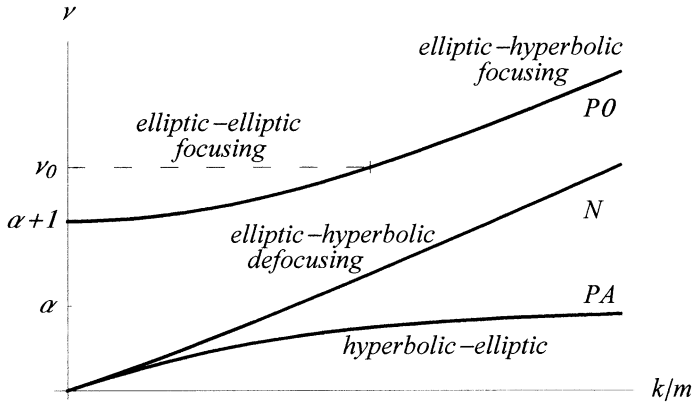

Figure 1. A plot of the dispersion relation, with mention of the classification of the DS models. Notice the threshold ν_0. The three branches are labelled PO, N, PA, for optical with positive helicity, negative helicity and acoustic with positive helicity, respectively. $\nu = \omega/m$ is a normalized frequency, m the saturation magnetization and α the ratio of the external field to m.

as $\alpha \to +\infty$. The approximation has been checked numerically, it is valid with a precision of better than 0.3% as soon as $\alpha \geqslant 2$. For small values of α,

$$\nu_0 = 1 + 1.25\alpha + 0.4375\alpha^2 + \mathrm{O}(\alpha^3). \tag{31}$$

This approximation has also been checked numerically, it is valid as soon as $\alpha \leqslant 0.7$, with the same precision as above.

The classification would be incomplete without mentioning the sign of the interaction constant r: it is positive on both the optical branches N and PO, and negative on the acoustic branch PA. The magnitude of the coefficients q and r is also of interest; the dependency of these coefficients with respect to the physical parameters α and ν is detailed in appendix B. The main features are the following: q tends to infinity for large k on the three branches, but is bounded anywhere else. It vanishes at the transition point $\nu = \nu_0$ on the PO branch. The order of magnitude of the bound is given by

$$q_m = \frac{1}{\sqrt{\alpha}} \pm \frac{1}{2\alpha} + \mathrm{O}\left(\frac{1}{\alpha\sqrt{\alpha}}\right). \tag{32}$$

The plus and minus signs hold, respectively, for the PA and PO branches, and q_m is a local minimum. The local maximum of q on the PO branch is reached at about $\nu = 3\alpha/2$, and is about $\frac{1}{4}$. More detailed and precise definitions are given in appendix B.

The interaction coefficient r vanishes for high frequencies ν on the PO and N branches, but also for low frequencies $\nu \simeq 0$ on the PA branch. Elsewhere its absolute value is bounded by 1, except near the point $k = 0$ of the optical branch, where it tends to infinity.

The signature of the operator $\mathcal{O}_3$, or rather of the operator $\mathcal{D}_3$ defined by $\mathcal{D}_3 \mathrm{e}^{\mathrm{i}\vec{k}\cdot\vec{x}} = -\mathcal{O}_3 \mathrm{e}^{\mathrm{i}\vec{k}\cdot\vec{x}}$, is easily determined using these results. It is definite negative on the PA branch and on the PO branch for $\nu < \nu_0$, and hyperbolic elsewhere. The fact that $|r| \leqslant 1$ intervenes in the justification of these features is, in a way, as important as the various signs. The condition for modulational stability given by [25] is $\mathcal{D}_1\mathcal{D}_2\mathcal{D}_3 > 0$ for all $\vec{k}$, where $\mathcal{D}_1$ and $\mathcal{D}_2$ are defined in the same way as $\mathcal{D}_3$. It is easily seen that this condition is never satisfied in the situation considered here: the system is always modulationally unstable, in the sense of [25]. In the same paper a condition for the existence of blow-up (called there self-focusing) is given, in the case where both $\mathcal{O}_1$ and $\mathcal{O}_2$ are elliptic (what we call elliptic–elliptic DS), thus definite

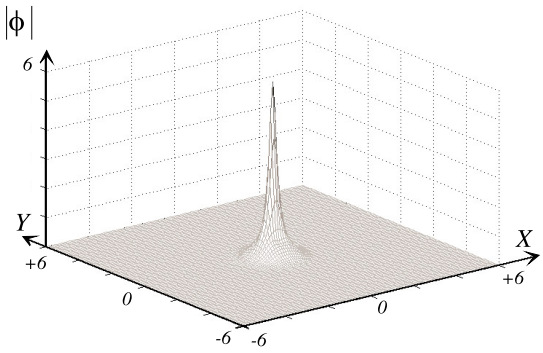

Figure 2. The elliptic–elliptic DS model for the positive optical wave: the pulse collapses after $T = 0.05$ propagation time. Initial data $\phi = 3\exp(-4(X^2 + Y^2))$. Parameters: $\alpha = 1$, $\nu = 2.2$, so that $q = 0.2$ and $r = 5$.

positive with their actual signs. When $\mathcal{O}_3$ is definite negative blow-up always occurs, when $\mathcal{O}_3$ is hyperbolic, blow-up may or may not occur. The former case occurs on the PO branch for $\nu < \nu_0$, as illustrated in figure 2.

4. Numerical computations

4.1. When the rectified field obeys an elliptic equation

4.1.1. Purpose and algorithm. Here we do not intend to make an extensive numerical study of the system derived in section 2, but only to give some examples of numerical solutions, in order to illustrate the above classification. Further, we restrict ourselves to $(2+1)$ dimensions, mainly because of the difficulties involved in the numerical resolution of the elliptic–hyperbolic system.

The algorithm used for the resolution of the elliptic–elliptic and hyperbolic–elliptic systems is rather simple. It reads as follows: we want to solve system (23), (24) with the initial data

$$\phi(X, Y, T = 0) = f(X, Y). \tag{33}$$

Notice that equation (24) does not involve initial Cauchy data for ψ but boundary values in the XY plane. We assume here that ψ vanishes at infinity. We build some recurrent sequence of functions ϕ_n, ψ_n, solving for each n the following Cauchy problem:

$$\begin{aligned} &\phi_{n+1}(X, Y, T = 0) = f(X, Y) \\ &(\mathrm{i}\partial_T + \partial_X^2 + \epsilon_1\partial_Y^2)\phi_{n+1} = -\epsilon_2\phi_n|\phi_n|^2 - r\phi_n\psi_n \\ &(q\partial_X^2 + \partial_Y^2)\psi_{n+1} = \partial_Y^2|\phi_{n+1}|^2. \end{aligned} \tag{34}$$

The equations of system (34) are linear and can be solved by Fourier analysis. We define the Fourier transform $\hat{F}$ of any function F by

$$\phi(X, Y, T) = \frac{1}{\sqrt{2\pi}} \int_{\mathbb{R}^2} \hat{\phi}(k, l, T)\mathrm{e}^{\mathrm{i}(kX+lY)}\,\mathrm{d}X\,\mathrm{d}Y. \tag{35}$$

Then system (34) is solved as

$$\widehat{\psi_{n+1}} = \frac{l^2}{qk^2 + l^2}\widehat{|\phi_{n+1}|^2} \tag{36}$$

$$\widehat{\phi_{n+1}} = \left[\hat{f} + \mathrm{i}\int_0^t (\epsilon_2\widehat{\phi_n|\phi_n|^2} + r\widehat{\phi_n\psi_n})\mathrm{e}^{\mathrm{i}(k^2+\epsilon_1 l^2)t'}\,\mathrm{d}t'\right]\mathrm{e}^{-\mathrm{i}(k^2+\epsilon_1 l^2)t}. \tag{37}$$

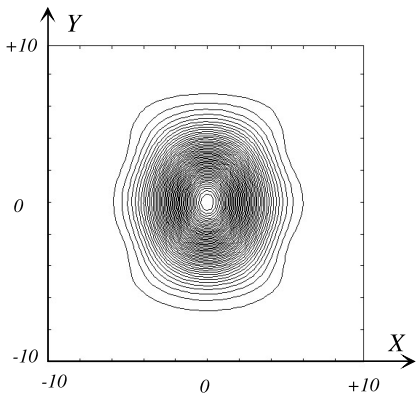

Figure 3. The hyperbolic–elliptic DS model for the positive acoustic wave: the pulse takes an elliptic shape when spreading out through diffraction and dispersion. Contour plot of $|\phi|$. Propagation time $T = 0.4$ and the initial data $\phi = 3\exp(-4(X^2+Y^2))$. Parameters: $\alpha = 1$, $\nu = 0.4$, so that $q = 1$ and $r = -0.625$.

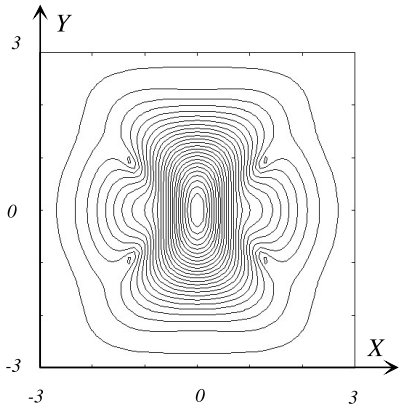

Figure 4. The hyperbolic–elliptic DS model for the positive acoustic wave: the unilateral focusing of the pulse. The parameters are the same as in figure 3, except the propagation time $T = 0.1$ and the initial data $\phi = 6\exp(-4(X^2 + Y^2))$.

The fixed point of the sequence $(\phi_n, \psi_n)_n$ is the solution of the Cauchy problem for system (23), (24). The above formulae are easily implemented on a PC using fast Fourier transforms. The numerical scheme converges quickly, but only for T values less than some bound, that decreases when the initial power grows. When this maximum is less than the desired propagation distance, the same scheme is repeated several times along the propagation.

4.1.2. Elliptic–elliptic case. On the PO branch, for normalized frequencies ν less than ν_0, the DS system is of the elliptic–elliptic type. The 1D reduction is focusing [17]. It has been shown [26] that it behaves similarly to the NLS model: when the energy of the pulse is small enough, it spreads out, while it blows up when the power input is sufficient. We present a set of evolution types almost all corresponding to the same Gaussian initial condition

$$\phi = 3\mathrm{e}^{-4(X^2+Y^2)}. \tag{38}$$

The external field strength is chosen so that $\alpha = 1$, and the normalized frequency is $\nu = 2.2$. Then the parameters of the DS system (23), (24) are $q \simeq 0.2$ and $r = 5$. At the short propagation time $T = 0.05$ one can see the beginning of the blow-up shown in figure 2. The long wave pulse emitted has the same shape as shown in figure 5, but with a much narrower size in relation to the main pulse size. It is known from [16] that damping will stop the blow up during the further propagation of the pulse.

4.1.3. Hyperbolic–elliptic case. On the PA branch, the type of DS system is hyperbolic–elliptic. The behaviour is not so simple because the wave is expected to be longitudinally self-focused, according to [17], but to be defocused transversely. Indeed, for the same initial data as above, the pulse takes indeed a non-circular shape, as shown in figure 3. However, the effect is not very strong, and the main behaviour is defocusing. A higher-power input can lead to pulse compression along one direction, as shown in figure 4. Some part of the total power moves away from the main peak, at its foot along the focusing direction, with a low intensity. This leads to the quadrilobate pulse shape seen in figure 4.

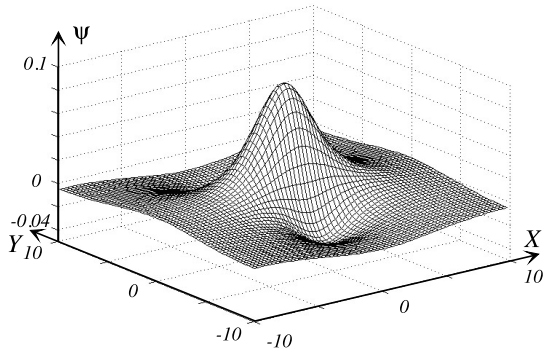

Figure 5. The hyperbolic–elliptic DS model for the positive acoustic wave: the typical shape of the emitted long wave ψ. This figure corresponds precisely to the high-frequency pulse shown in figure 3.

The emitted long wave corresponding to the pulse of figure 3 is plotted in figure 5. It presents a central positive peak, and two smaller negative ones, on both its sides. This characteristic shape seems to occur for most localized pulses when the second equation of the DS system (23), (24) is elliptic. It size obviously depends on the size of the high-frequency pulse, but also on the q parameter. For large values of q, as occurs on the PA branch when the wavenumber is large, the size of the long wave pulse along the X-axis becomes huge. At the limit $q \to +\infty$ this pulse becomes almost 1D, modulated along the Y direction only.

4.2. When the rectified field obeys an hyperbolic equation

4.2.1. Another numerical scheme. The second equation (24) of the DS system, governing the evolution of the rectified field, is hyperbolic for the waves with negative helicity, and on the PO branch for normalized frequencies higher than ν_0. This hyperbolicity strongly modifies the behaviour of the whole system.

First, the numerical scheme presented in the section above does not yield a resolution of the elliptic–hyperbolic DS system, because when q is negative, formula (36) is singular. In fact, the hyperbolic character of the second equation (24) of the system radically changes the allowed boundary conditions for ψ. Due to propagation along the directions $X \pm \sqrt{-q}Y$, ψ cannot be set to a fixed value in both the cases $X, Y \to -\infty$ and $X, Y \to +\infty$. A numerical scheme is given in [9], it works as follows: the rectified field ψ is replaced by a primitive Ψ such that $\partial_Y \Psi = \psi$, and the characteristics of the hyperbolic operator are taken as new variables $\tilde{X} = X - cY$ and $\tilde{Y} = X + cY$; $c = \sqrt{-q}$ is the velocity of this propagation mode in the frame that moves with the high-frequency pulse (take care to avoid confusion with light velocity, light velocity in the medium in denoted by c_0 in the paper). Equations (23), (24) are transformed into

$$[\mathrm{i}\partial_T + (1-q)(\partial_{\tilde{X}}^2 + \partial_{\tilde{Y}}^2) + 2(1+q)\partial_{\tilde{X}}\partial_{\tilde{Y}}]\phi + \epsilon_2\phi|\phi|^2 - rc\phi(\partial_{\tilde{X}} - \partial_{\tilde{Y}})\Psi = 0 \tag{39}$$

$$\partial_{\tilde{X}}\partial_{\tilde{Y}}\Psi = \frac{1}{4c}(\partial_{\tilde{X}} - \partial_{\tilde{Y}})|\phi|^2. \tag{40}$$

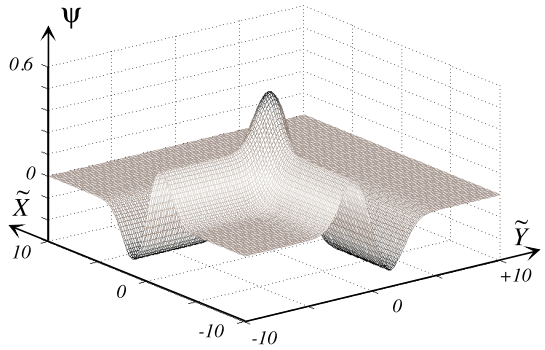

Figure 6. The elliptic–hyperbolic DS model for the wave with negative helicity: the typical shape of the emitted long wave ψ. Propagation time $T = 0.16$ and the initial data $\phi = 3\exp(-4(X^2+Y^2))$. Boundary values: $\psi_1(\tilde{X}) \equiv 0$, $\psi_2(\tilde{Y}) \equiv 0$. Parameters: $\alpha = 1$, $\nu = 0.5$ so that $c = \sqrt{-q} = 1.5$ and $r = 0.4$.

The initial and boundary conditions are

$$\begin{aligned} &\phi(\tilde{X},\tilde{Y},0) = f(\tilde{X},\tilde{Y}) \\ &\lim_{\tilde{Y}\to+\infty} \Psi(\tilde{X},\tilde{Y},T) = \Psi_1(\tilde{X},T) \\ &\lim_{\tilde{X}\to+\infty} \Psi(\tilde{X},\tilde{Y},T) = \Psi_2(\tilde{Y},T). \end{aligned} \tag{41}$$

The two boundary conditions can be expressed in a simple way when discretizing on a square grid, and the discrete version of the propagation equation (40) for Ψ can be solved by an explicit computation at each step, assuming that the required value of ϕ is known. Equation (39) is then solved by a fixed-point method, using finite differences.

4.2.2. Boundary conditions. The boundary conditions (41) have been slightly modified with regard to [9], in order to respect causality in the present physical situation. Indeed, according to the scaling, the characteristic variables $\tilde{X}$ and $\tilde{Y}$ of the hyperbolic equation read

$$\begin{aligned} \tilde{X} &= \varepsilon\left(x - Vt - c\sqrt{\left|\frac{B}{C}\right|}y\right) \\ \tilde{Y} &= \varepsilon\left(x - Vt + c\sqrt{\left|\frac{B}{C}\right|}y\right). \end{aligned} \tag{42}$$

Thus the limits as $\tilde{X} \to +\infty$ or $\tilde{Y} \to +\infty$ involved by the boundary conditions (41) correspond to the past: $t \to -\infty$. The physical phenomenon that arises here has already been considered in [28]: the fast-oscillating wave emits a 'low-frequency' wave, correctly speaking, a solitary long wave. This solitary wave propagates isotropically in space with its own velocity, and two situations can arise: when the emitted wave travels faster than the main pulse, it stays around it, and accompanies it. When the emitted wave travels slower than the main pulse, it is left behind it and concentrates on a cone analogously to a supersonic boom. In (2 + 1) dimensions, this is described by the elliptic–hyperbolic DS system, with vanishing boundary conditions $\Psi_1 \equiv 0$ and $\Psi_2 \equiv 0$. A sample of the corresponding emitted long wave is plotted in figure 6. The behaviour of the main pulse is not significantly modified with respect to the elliptic–elliptic case, for these vanishing boundary conditions.

Nonvanishing boundary conditions give rise to a set of pulse behaviours, some of which are rather exotic. Before presenting a sample of these behaviours, let us precise the physical interpretation of these boundary conditions. Notice first that the numerical scheme of [9] involves boundary values $\Psi_1(\tilde{X})$ and $\Psi_2(\tilde{Y})$, for the quantity Ψ that appears in equations (39), (40), while the quantity that has a physical meaning is $\psi = \partial_Y \Psi$, indeed

$$\psi = \frac{-F}{G}\sqrt{\left|\frac{D}{B}\right|}(H_2^{0,x} + M_2^{0,x}) \tag{43}$$

where $H_2^{0,x} + M_2^{0,x} = B_2^{0,x}$ is a component of the magnetic field. The boundary values corresponding to ψ are $\psi_1 = -c\frac{\mathrm{d}\Psi_1(\tilde{X})}{\mathrm{d}\tilde{X}}$ and $\psi_2 = c\frac{\mathrm{d}\Psi_2(\tilde{Y})}{\mathrm{d}\tilde{Y}}$.

ψ_1 and ψ_2 are limits of ψ as $t \to -\infty$, or according to (42), as $x \to +\infty$. Indeed, because the main pulse travels faster that these waves, the initial state of the latter, corresponding to the past, is located in front of the former. ψ_1 obviously describes a wave propagating at the speed $+c$ in the Y direction in the XY frame that moves with the main pulse. It is interesting to compute its velocity with regard to the xy frame of the laboratory. First, expression (22) of c reduces equation (42) to

$$\tilde{X} = \varepsilon V\left(\frac{y}{V\sqrt{|F|}} + \frac{x}{V} - t\right). \tag{44}$$

The value of the speed follows from (44), it reads

$$\vec{V}_1 = \frac{V\sqrt{|F|}}{1+|F|}(1, \sqrt{|F|}). \tag{45}$$

In the same way, ψ_2 represents a wave propagating at speed $-c$ in the moving frame and $\vec{V}_2 = \frac{V\sqrt{|F|}}{1+|F|}(\sqrt{|F|}, -1, 0)$ in the lab frame. The tips of the speed vectors $\vec{V}_1$ and $\vec{V}_2$ belong to a circle whose diameter is $[(0, 0), (V, 0)]$ in the xy plane. These vectors make an angle θ with the x-axis, that is the direction of the group velocity $\vec{V}$ of the main pulse, so that $\cot\theta = \sqrt{|F|}$. According to (22), q is zero when F is infinite. Thus the frequency threshold ν_0 between the situations where equation (24) is either elliptic or hyperbolic on the PO branch corresponds to an angle $\theta = 0$, i.e. to $\|\vec{V}_1\| = V_1^x = V$. $\|\vec{V}_1\|$ and V_1^x are always smaller than V in the hyperbolic case, becoming equal to it at the threshold. The speed of the considered propagation mode should be greater than V in the elliptic case, according to the above interpretation.

The model therefore describes a three-wave interaction, between the high-frequency wave propagating at speed V and the two 1D long waves described by $\psi_1(\tilde{X})$ and $\psi_2(\tilde{Y})$. The geometry of the problem, and the interpretation of the boundary values $\psi_1(\tilde{X})$ and $\psi_2(\tilde{Y})$ as free incident waves are illustrated in figure 7. Notice that not all long waves can interact with the high-frequency pulse. The polarization is fixed: it must be along the x-axis, as can be seen through definition (43) of ψ. Second, the propagation direction must be the same as the direction in which the high-frequency pulse can emit a long wave. This yields a kind of resonance. In fact, any point of the matched plane long wave will see the high-frequency pulse and interact with it, because in the frame moving with the high-frequency pulse, the plane long wave travels parallel to its own plane, and seems motionless.

4.2.3. Defocusing case. The self-interaction of the wave with negative helicity is defocusing. For vanishing boundary values, the interaction with the rectified field ψ does not appreciably modify the behaviour of the input pulse. But a nonzero value of ψ at infinity, that is, nonzero incident waves $\psi_1(\tilde{X})$ and $\psi_2(\tilde{Y})$, can strongly modify the behaviour. The result obviously depends on the input, especially on the signs of $\psi_1(\tilde{X})$ and $\psi_2(\tilde{Y})$. For negative ψ_1 and

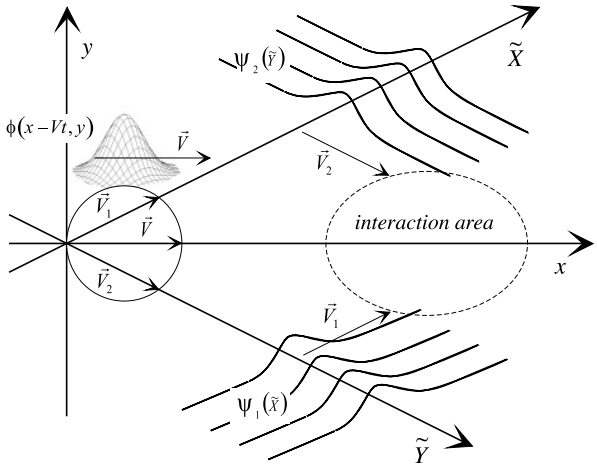

Figure 7. The hyperbolic–elliptic DS model: geometry and boundary values interpretation. The incident long waves described by $\psi_1(\tilde{X})$ and $\psi_2(\tilde{Y})$ travel with the speeds $\vec{V}_1$ and $\vec{V}_2$ respectively. The high-frequency wave is localized, and travels at speed $\vec{V}$. Because V is greater than V_1 and V_2, and the velocities are matched, the three waves arrive in the interaction area simultaneously, and interaction can occur.

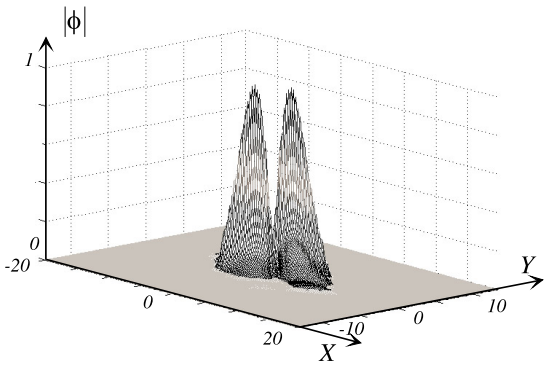

Figure 8. The elliptic–hyperbolic DS model for the wave with negative helicity: splitting of a single pulse into two through interaction with long waves. Propagation time $T = 0.36$ and the initial data $\phi = 3\exp(-4(X^2 + Y^2))$. Boundary values: $\psi_1(\tilde{X}) = -60/\cosh^2(4\tilde{X})$, $\psi_2(\tilde{Y}) = +60/\cosh^2(4\tilde{Y})$. Parameters: $\alpha = 1$, $\nu = 0.5$ so that $c = \sqrt{-q} = 1.5$ and $r = 0.4$.

positive ψ_2, the Gaussian input pulse can be cut into two parts (see figures 8 and 9). Consider the contour plot presented in figure 9: the energy of the wave $\psi_2(\tilde{Y})$ concentrates about the first diagonal $\tilde{Y} = X - cY = 0$, while the energy of the other wave $\psi_1(\tilde{X})$ concentrates about the second diagonal $\tilde{X} = X + cY = 0$. ψ_1 being negative yields an interaction factor $r\psi$ which is negative at this point (r is positive on both the N and the PO branches), and thus corresponds to a defocusing interaction. The positive ψ_2 yields a focusing interaction about the first diagonal. The pulse energy focuses and concentrates about the first diagonal, while its amplitude takes very low values, along the second one, where defocusing occurs. Finally, the interaction between the pulse and the long wave ψ appears to be repulsive in the region where $\psi < 0$, and attractive in the region where $\psi > 0$.

Another example is given by figure 10: with the same parameters and initial and boundary

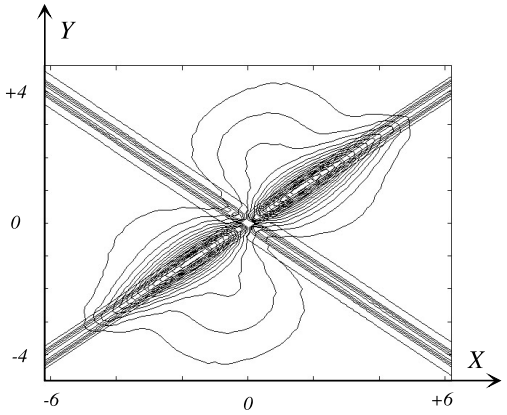

Figure 9. The elliptic–hyperbolic DS model for the wave with negative helicity: splitting of a single pulse into two. Contour plot of both the high-frequency pulse and the long waves interacting together. All the parameters, initial and boundary data are the same as in figure 8.

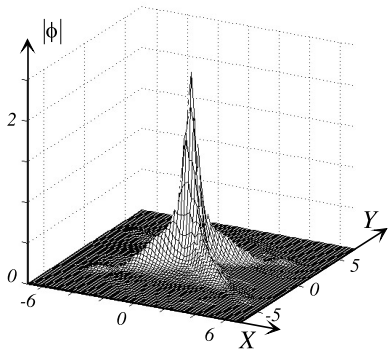

Figure 10. The elliptic–hyperbolic DS model for the wave with negative helicity: the interaction prevents the pulse from spreading out. Notice the pointed end. All parameters, initial and boundary data are the same as in figure 8, except that $\psi_1(\tilde{X}) = +60/\cosh^2(4\tilde{X})$.

data, except a sign change of ψ_1, so that both boundary values of ψ are positive, and thus the whole interaction is focusing. The peak is very sharp, and the interaction has partially prevented it from spreading out. The peak height is indeed still 2.4 (in normalized units, according to the above variable changes) in figure 10 after a propagation time of $T = 0.36$, instead of 0.5 in the linear case. Here the focusing also gives rise to an attractive effect. The pulse energy concentrates on the point where ψ is positive, giving rise to a rather particular four-branch star shape. Further, the focusing is stronger at the point where the two long waves cross one another, so that the pulse ends with a pointed tip.

A change in the length of the long wave pulses ψ_1 and ψ_2 modifies the behaviour of the main pulse. Figure 11 shows a contour plot of both the high-frequency pulse and long waves, for values of ψ_1 and ψ_2 concentrated on much shorter peaks. Instead of the four-branch star of figure 10, the pulse takes the shape of a square, whose sides are approximately parallel to the X and Y axes. The spreading out occurs despite the interaction, only the pointed tip still exists.

4.2.4. Focusing case. The self-interaction of the PO wave is focusing. For normalized frequencies $\nu > \nu_0$, the modulation evolution is described by an elliptic–hyperbolic DS system. As in the defocusing case, the interaction with the emitted long wave does not modify the behaviour of the high-frequency pulse in an important way. For low-power input, the pulse is spread out, while it collapses when the power input is higher.

First we consider an input pulse whose energy is not sufficient for collapse. If the incident long waves $\psi_1(\tilde{X})$ and $\psi_2(\tilde{Y})$ are large enough and positive, the interaction can lead to a stabilization of the pulse. The wave interaction is then focusing ($r > 0$), and can balance the defocusing effects of both self-interaction and diffraction–dispersion. An example of such stabilization is given in figure 12.

Figure 13 presents the shape of the long wave, in this special situation. It can be noticed, through an attentive study of the figure, that the maximal wave amplitude is slightly higher after the interaction than before. The central peak is mainly the sum of the two waves.

Taking a higher-power input leads *a priori* to collapse. Is it possible that the interaction

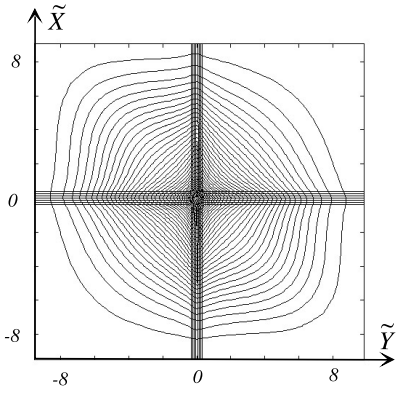

Figure 11. The elliptic–hyperbolic DS model for the wave with negative helicity: an initially round pulse takes a square shape. Contour plot of both the high-frequency pulse and the long waves interacting together. The coordinates are characteristic of the hyperbolic equation: $\tilde{X} = X + cY$, $\tilde{Y} = X - cY$. The parameters and initial data are the same as in figure 8. The boundary values are $\psi_1(\tilde{X}) = +45/\cosh^2(15\tilde{X})$, $\psi_2(\tilde{Y}) = +45/\cosh^2(15\tilde{Y})$.

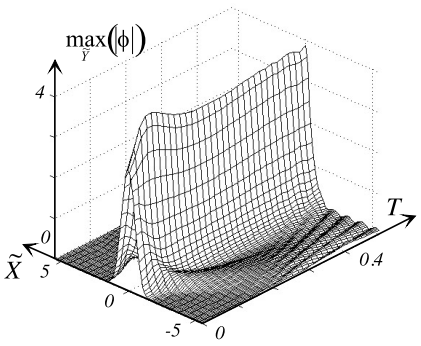

Figure 12. The elliptic–hyperbolic DS model for the wave with positive helicity: stabilization of a pulse through interaction with long waves. The figure presents the evolution during propagation (variable T) of some $\tilde{X}$-cut profile of the 2D pulse, precisely defined by: $\max_{\tilde{Y}}(|\phi(\tilde{X}, \tilde{Y}, T)|)$. Initial data $\phi = 3\exp(-4(X^2 + Y^2))$. Boundary values: $\psi_1(\tilde{X}) = 32/\cosh^2(4\tilde{X})$, $\psi_2(\tilde{Y}) = 32/\cosh^2(4\tilde{Y})$. Parameters: $\alpha = 1$, $\nu = 3.65$ so that $c = \sqrt{-q} = 1$ and $r = 0.6$. (The oscillations after $T = 0.4$ are due to reflections of the wave on the numerical box boundary, these reflected waves can be seen at the upper-right side of the plot.)

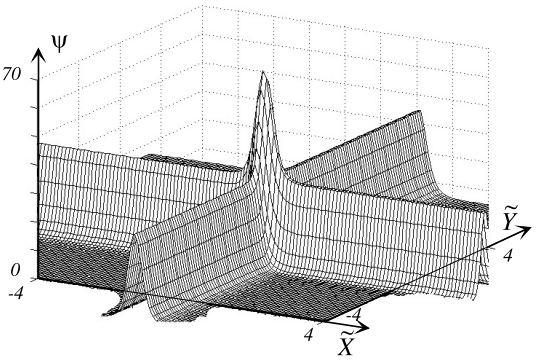

Figure 13. The elliptic–hyperbolic DS model for the wave with positive helicity: the shape of the long waves. Initial data, boundary values and parameters are the same as in figure 12. Propagation time $T = 0.4$.

with the long wave prevents the collapse? A remarkable situation is shown in figure 14. Through defocusing interaction with adequate value of the incident long waves, (indeed, as above, the behaviour depends crucially on the sign of the latter), the initial Gaussian pulse is cut into four parts. The energy of each part is less than that required for collapse, and collapse is avoided here. Further evolution of the pulses shows, besides their spreading out, that they continue to move away from each other.

5. Conclusion

The model that describes the evolution of some localized electromagnetic pulse in a saturated ferromagnetic bulk medium has been derived. It is a 3D version of the DS system, with an additional damping term. The behaviour of the solutions of this system is expected to depend on co-

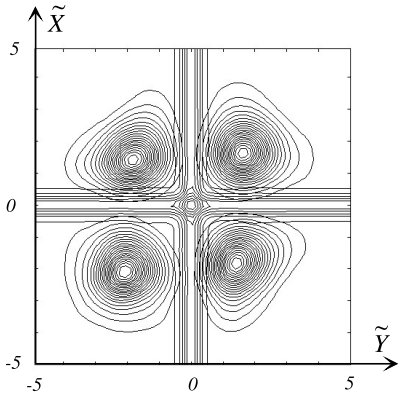

Figure 14. The elliptic–hyperbolic DS model for the wave with positive helicity: an initially Gaussian pulse is cut into four parts through interaction with long waves. Initial data $\phi = 6/\exp(-4(X^2 + Y^2))$. Boundary values: $\psi_1(\tilde{X}) = -100/\cosh^2(4\tilde{X})$, $\psi_2(\tilde{Y}) = -100/\cosh^2(4\tilde{Y})$. The parameters are the same as in figure 12. Propagation time $T = 0.15$.

efficient values, that have been classified according to the usual classification of the DS system.

Most of the possible situations occur, it only fails in the hyperbolic–hyperbolic and the elliptic–elliptic defocusing cases. It has been seen that the (2 + 1)-dimensional reduction with negligible damping (the DS system) is never integrable by means of the IST method in the considered situation. Examples of numerical resolution of this (2 + 1)-dimensional reduction have been given in order to illustrate every case of the classification. The behaviour is mainly the same as that of the corresponding 2D NLS model, showing collapse for the 'optical' wave with positive helicity, or spreading out. Focusing in the transverse direction while the pulse is defocused in the longitudinal direction also occurs in the hyperbolic–elliptic situation. This occurs for the waves of the PA branch, that are mainly the MSW. Notice that blow-up, corresponding to an elliptical equation, has been observed in YIG thin films: the difference can be explained by the fact that the present work would describe thick films, with a thickness of the same order of magnitude as the pulse width.

Very interesting and surprising behaviour can arise due to the interaction between the pulse and incident long waves, described by the elliptic–hyperbolic DS model. The initial pulse can be cut into two of four parts, spread-out or collapse can be prevented at least partially, and even pulse stabilization is possible. The examples always consider two symmetrical incident long waves, to preserve the analogy with the dromion solutions of the completely integrable situation. The case of a single incident wave is to be investigated in a more systematic study of the system, together with the resolution of the 3D case. These effects are obtained on the PO and N branches, that is, for the proper EM waves. From the experimental point of view, the result has two drawbacks: first, because of the frequency dependence of the coupling coefficient r (equation (86)), the efficiency of the interaction decreases for high frequencies. Thus the observation of the effects for infrared frequencies would involve higher-power input for the long waves. Second, the lower frequencies, close to the ferromagnetic resonance frequency (polaritons), involve rather long wavelengths. However, the pulse length must be large with respect to the wavelength, and the propagation length large with respect to the pulse length, thus the sample size needed could become huge. It is thought that an adequate balance between these two points would allow the observation of the predicted effects.

It must be noticed that, in the absence of incident matched long waves, the solutions of the DS system do not differ qualitatively from those of the 2D NLS equation. Thus the experimental results that were correctly described in a phenomenological way by the 2D NLS equation are in good agreement with the present theory. The latter has the advantage of being more rigorous from the mathematical point of view, which is interesting in itself, and can lead to better quantitative results. The three-wave interaction described by the elliptic–hyperbolic

DS system should be observable, and may lead to applications. Besides this, it must be noted that the DS system is a very general model, that describes the nonlinear evolution of wave modulation in quadratic nonlinear media in a wide range of physical contexts. Therefore, the pulse behaviours reported in this paper are expected to occur in other physical situations. The analogue of these phenomena in the frame of nonlinear optics, would especially lead to applications of major interest, including the possibility of beam control.

Acknowledgments

The author is indebted to Professor M A Manna, who provided him with the basic ideas which lead to this paper, and checked all the computations involved by the multiscale expansion. He has refused to be the co-author of the paper, due to his great modesty.

Appendix A. Details of the multiscale analysis

A.1. Derivation of the evolution equation for the fundamental wave amplitude

At second order, the equations regarding the fundamental frequency $n = 1$ yield, as a compatibility condition, the value of the velocity

$$V = u\left(1 + \frac{\delta\nu}{2\Omega(\Omega+1) - \delta\nu}\right) \tag{46}$$

where $u = \omega/k$ is the phase velocity. In this expression and what follows, the parameter

$$\Omega = \alpha + \delta\nu \tag{47}$$

is used for convenience.

The second-order terms in the expansion read as

$$\vec{H}_2^1 = \begin{pmatrix} \frac{ik}{\omega^2}(\mathrm{i}\delta\partial_\eta + \partial_\zeta)g \\ \mathrm{i}\delta f \\ f \end{pmatrix} \qquad \vec{M}_2^1 = -(\gamma f + \mathrm{i}\Lambda\partial_\xi g)\begin{pmatrix} 0 \\ \mathrm{i}\delta \\ 1 \end{pmatrix} \tag{48}$$

where f is an unknown function, the analogue to g belonging to this second order. The constant is given by

$$\Lambda = \frac{-2\delta}{um}\frac{1}{2\Omega(\Omega+1) - \delta\nu}. \tag{49}$$

The terms $\vec{H}_2^2$ and $\vec{M}_2^2$ vanish, while the equations for the zero-harmonic or mean-value terms $\vec{H}_2^0$ and $\vec{M}_2^0$ are to be partly sought at a higher order, see the next section.

The compatibility condition at order ε^3 for the fundamental the frequency term yields the evolution equation (12) for g, the computation is detailed below. The equations coming from (2) are reduced by lengthy but straightforward calculation to

$$H_3^{1,x} + M_3^{1,x} = \frac{1}{\omega^2}\left(1 - 2\frac{V}{u}\right)\partial_\xi(\mathrm{i}\delta\partial_\eta + \partial_\zeta)g + \frac{\mathrm{i}k}{\omega^2}(\mathrm{i}\delta\partial_\eta + \partial_\zeta)f \tag{50}$$

$$\gamma H_3^{1,y} + M_3^{1,y} = \mathrm{i}\delta\Theta - \left[\frac{\mathrm{i}\delta}{\omega^2}\partial_\zeta + \frac{k^2}{\omega^4}\partial_\eta\right](\mathrm{i}\delta\partial_\eta + \partial_\zeta)g \tag{51}$$

$$\gamma H_3^{1,z} + M_3^{1,z} = \Theta + \left[\frac{\mathrm{i}\delta}{\omega^2}\partial_\eta - \frac{k^2}{\omega^4}\partial_\zeta\right](\mathrm{i}\delta\partial_\eta + \partial_\zeta)g \tag{52}$$

with

$$\Theta = \theta_1 \partial_\xi f + \theta_2 \partial_\tau g + \theta_3 \partial_\xi^2 g \tag{53}$$

$$\theta_1 = \frac{2\mathrm{i}\delta}{um} \frac{1}{2\Omega(\Omega+1) - \delta\nu} \tag{54}$$

$$\theta_2 = \frac{-2\mathrm{i}}{m\nu} \frac{(\Omega+1)}{\Omega} \tag{55}$$

$$\theta_3 = \frac{-\delta}{m^2\nu} \frac{4\Omega(\Omega+1) + \delta\nu}{[2\Omega(\Omega+1) - \delta\nu]^2}. \tag{56}$$

The importance of the operator $\partial_\perp = \mathrm{i}\delta\partial_\eta + \partial_\zeta$ appears in these equations.

The expressions of the $\vec{M}_3^1$ components derived directly from equations (50)–(52) are reported in the equation coming from the Landau equation (1) at this third order

$$\vec{m} \wedge (\vec{H}_3^1 - \alpha \vec{M}_3^1) - \mathrm{i}\omega \vec{M}_3^1 = V \partial_\xi \vec{M}_2^1 - \partial_\tau \vec{M}_1^1 - (\vec{M}_1^1 \wedge \vec{H}_2^0 + \vec{M}_2^0 \wedge \vec{H}_1^1) + \frac{\hat{\sigma}}{\|\vec{M}_0^0\|} \vec{M}_0^0 \wedge (\vec{M}_0^0 \wedge \vec{H}_1^1 + \vec{M}_1^1 \wedge \vec{H}_0^0). \tag{57}$$

Let us call $\vec{J}$ and $\vec{K}$, respectively, the left- and the right-hand sides of equation (57). The compatibility condition is obtained by eliminating $H_3^{1,y}$ and $H_3^{1,z}$ from the y and z components of equation (57). It reads

$$J_0^y + \mathrm{i}\delta J_0^z = K^y + \mathrm{i}\delta K^z \tag{58}$$

where J_0^y and J_0^z are the parts of the corresponding $\vec{J}$ components that do not contain the components of $\vec{H}_3^1$. Explicit computation of the two members of equation (58) using all the above expressions yields evolution equation (11).

A.2. Derivation of the equations governing the behaviour of the zero-frequency term

At order ε^4, for the so-called mean-value or zero-harmonic fields $\vec{H}_2^0$ and $\vec{M}_2^0$, the Maxwell equations yield

$$\partial_\xi^2(\vec{H}_2^{0,x} + \vec{M}_2^{0,x}) = \frac{1}{V^2}(\partial_\eta^2 + \partial_\zeta^2)\vec{H}_2^{0,x} - \frac{1}{V^2}\partial_\xi(\partial_\eta \vec{H}_2^{0,y} + \partial_\zeta \vec{H}_2^{0,z}) \tag{59}$$

$$\partial_\xi^2(\beta\vec{H}_2^{0,y} + \vec{M}_2^{0,y}) = \frac{1}{V^2}\partial_\zeta^2 \vec{H}_2^{0,y} - \frac{1}{V^2}\partial_\eta(\partial_\xi \vec{H}_2^{0,x} + \partial_\zeta \vec{H}_2^{0,z}) \tag{60}$$

$$\partial_\xi^2(\beta\vec{H}_2^{0,z} + \vec{M}_2^{0,z}) = \frac{1}{V^2}\partial_\eta^2 \vec{H}_2^{0,z} - \frac{1}{V^2}\partial_\zeta(\partial_\xi \vec{H}_2^{0,x} + \partial_\eta \vec{H}_2^{0,y}). \tag{61}$$

We set $\beta = 1 - \frac{1}{V^2}$. This can be reduced in the following way: first the equations are integrated twice, and three new unknown functions Φ, Φ', Φ'' are defined, which are equal, respectively, to the right-hand side members of these equations. This yields a simple expression of the components of $\vec{M}_2^0$ in terms of those of $\vec{H}_2^0$ and these $\Phi^{(j)}$. This expression can be used in the Landau equation at order ε^2:

$$\vec{m} \wedge (\vec{H}_2^0 - \alpha \vec{M}_2^0) = -(\vec{M}_1^1 \wedge \vec{H}_1^{1*} + \vec{M}_1^{1*} \wedge \vec{H}_1^1). \tag{62}$$

Notice that this equation does not contain any damping term, since we assume that the damping constant $\tilde{\sigma}$ has an order of magnitude of ε^2, according to equation (6). The expressions for $\vec{M}_2^0$ and $\vec{H}_2^0$ then read

$$\vec{H}_2^0 = \begin{pmatrix} \Xi \\ \frac{\alpha}{1+\alpha\beta}\Phi' \\ \frac{\alpha}{1+\alpha\beta}\Phi'' \end{pmatrix} \qquad \vec{M}_2^0 = \begin{pmatrix} -\Xi + \Phi \\ \frac{1}{1+\alpha\beta}\Phi' \\ \frac{1}{1+\alpha\beta}\Phi'' \end{pmatrix}. \tag{63}$$

An additional equation governing the behaviour of these terms is obtained at order ε^3 in the Landau equation. It is the compatibility condition at this order, and reads

$$\vec{m} \cdot \left[V \partial_\xi \vec{M}_2^0 - \sum_{p+q=0} (\vec{M}_1^p \wedge \vec{H}_2^q + \vec{M}_2^p \wedge \vec{H}_1^q) \right] = 0. \tag{64}$$

Making use of the previous results, especially equation (63), in equation (64) yields

$$\Xi = \Phi - 2\delta \frac{\Lambda}{V} (|g|^2 - \rho^2) \tag{65}$$

where ρ^2 is an arbitrary function of the variables (η, ζ, τ) only. If $\vec{M}_2^0$ is assumed to vanish as $\xi \to -\infty$, it satisfies

$$\rho^2 = \lim_{\xi \to -\infty} |g|^2. \tag{66}$$

Because only Φ, but not Φ' nor Φ'', appears in evolution equation (11) for g, we are only interested in the equation governing the evolution of this field. The equations for the three $\Phi^{(j)}$ are straightforwardly derived from equations (59)–(61). The components of $\vec{H}_2^0$ and $\vec{M}_2^0$ are eliminated from these equations, using equation (10), and the definition of $\Phi^{(j)}$. Indeed, the left-hand side of equation (59) is exactly $\partial_\xi^2 \Phi$, and so on. An adequate combination of equations (60) and (61) shows that

$$\partial_\xi^2 (\partial_\eta \Phi' + \partial_\zeta \Phi'') = \frac{-1}{V^2} \partial_\xi (\partial_\eta^2 + \partial_\zeta^2) H_2^{0,x}. \tag{67}$$

After integration with respect to ξ, relation (67) allows the elimination of Φ' and Φ'' from equation (59), yielding equation (12) that governs the evolution of Φ.

A.3. Expression of the coefficients

The above computation gives explicit expressions for all the coefficients involved in equations (11) and (12). All these expressions are listed below, they are used for the classification given in section 3. We make use of the parameter $\Omega = \alpha + \delta\nu$, for short-hand notation:

$$A = \frac{2}{\delta\nu\Omega} (2\Omega(\Omega + 1) - \delta\nu) \tag{68}$$

$$B = \frac{2\Omega(4\alpha(\Omega + 1) + \delta\nu)}{m\nu(2\Omega(\Omega + 1) - \delta\nu)^2} \tag{69}$$

$$C = \frac{\delta}{m\nu^2} (2\Omega + 1) \tag{70}$$

$$D = \frac{-4\delta(\Omega + 1)}{m\Omega^3} \tag{71}$$

$$E = \frac{-2\delta}{\Omega} \tag{72}$$

$$F = \frac{(1 + \alpha)(2\Omega(\Omega + 1) - \delta\nu)^2}{4(1 + \alpha)\Omega^3(\Omega + 1) - \alpha(2\Omega(\Omega + 1) - \delta\nu)^2} \tag{73}$$

$$G = \frac{2}{m\Omega^2} F \tag{74}$$

$$\Sigma = -2\tilde{\sigma} m \frac{\delta\nu}{\Omega}. \tag{75}$$

Appendix B. Study of the coefficients of the reduced DS-type system

B.1. Study of ϵ_2

The first sign is $\epsilon_1 = \mathrm{sgn}\,(BD)$. It has been studied in detail in [17]. Precisely, the NLS equation derived in [17] can be presented as

$$\mathrm{i}\tilde{A}\partial_\tau \tilde{g} + \tilde{B}\partial_\xi^2 \tilde{g} + \tilde{C}\tilde{g}|\tilde{g}|^2 = 0. \tag{76}$$

We use the sign $(\tilde{\ })$ in order to avoid confusion between the notation of the present paper and that of [17]. Normalizations are indeed slightly different. We have

$$\tilde{A} = \frac{-m^3\nu^3}{\Omega^2}A \qquad \tilde{B} = \frac{-m^3\nu^3}{\Omega^2}B \qquad \tilde{C} = \frac{-m^5\nu^5}{\Omega^4}D. \tag{77}$$

It is then straightforward to see that $\mathrm{sgn}\,(BD) = \mathrm{sgn}\,(\tilde{B}\tilde{C})$. The result of [17] is thus valid, it reads

$$\epsilon_2 = -\delta. \tag{78}$$

B.2. Study of ϵ_1

ϵ_1 is determined as follows. We first note that $\epsilon_1\epsilon_2 = \mathrm{sgn}\,(CD)$, and that the product CD factorizes, using expressions (70) and (71). Thus

$$\epsilon_1\epsilon_2 = -\mathrm{sgn}\,(\Omega(\Omega+1)(2\Omega+1)). \tag{79}$$

For the wave with negative helicity, $\delta = +1$, ν takes any positive value, thus $\Omega > \alpha$, and $\epsilon_1\epsilon_2 < 0$, thus $\epsilon_1 > 0$. The dispersion relation presents two branches describing waves with positive helicity and $\delta < 0$. The acoustic branch PA corresponds to normalized frequencies ν belonging to $]0, \alpha[$, while the optical branch PO corresponds to $\nu > (1+\alpha)$. Elementary analysis shows that $\epsilon_1\epsilon_2$ is negative on the acoustic branch and positive on the optical one. The value of ϵ_1 follows directly.

B.3. Sign of the q coefficient

From the definitions (22) it is easily seen that $\mathrm{sgn}\,(q) = -\mathrm{sgn}\,(F)$, and from (73) that the sign of F is the sign of its denominator. Let us call $-\mathcal{L}$ this denominator, so that $\mathrm{sgn}\,(q) = \mathrm{sgn}\,(\mathcal{L})$. It factorizes into

$$\mathcal{L} = -\delta\nu(\alpha^2 + 4\Omega^2(\Omega+1) + \alpha\Omega(3+4\Omega)). \tag{80}$$

For $\delta = +1$, Ω is always positive, as is α, thus q is negative. For $\delta = -1$, on the acoustic branch, Ω is still positive, thus $q > 0$. But on the optical branch, $\Omega < -1$, and a sign change can be expected. Indeed, the polynomial $P_\alpha(\Omega) = \alpha^2 + 4\Omega^2(\Omega+1) + \alpha\Omega(3+4\Omega)$ tends to $-\infty$ as $\Omega \to -\infty$, and $P_\alpha(-1)$ is positive. Thus it admits one or three zeros in the considered interval.

The theory of algebraic resolution of the third-degree equation applies as follows: the transform $\mathcal{W} = \Omega + (1+\alpha)/3$ reduces the equation $P_\alpha(\Omega) = 0$ to $\mathcal{W}^3 + P\mathcal{W} + Q = 0$, with $P = -(4\alpha^2 - \alpha + 4)/12$ and $Q = (8\alpha^3 + 24\alpha^2 - 3\alpha + 8)/108$. The discriminant is $\Delta = 4P^3 + 27Q^2 = \alpha^2(16\alpha^3 + 12\alpha^2 + 3\alpha + 7)/16$. For $\alpha > 0$, Δ is always positive, thus the equation admits a unique real solution Ω_0. It reads

$$\Omega_0 = -\tfrac{1}{6}\left(\sqrt[3]{8 - 3\alpha + 24\alpha^2 + 8\alpha^3 + 3\sqrt{3}\alpha\sqrt{7 + 3\alpha + 12\alpha^2 + 16\alpha^3}}\right.$$
$$\left. + \sqrt[3]{8 - 3\alpha + 24\alpha^2 + 8\alpha^3 - 3\sqrt{3}\alpha\sqrt{7 + 3\alpha + 12\alpha^2 + 16\alpha^3}} + 2(1+\alpha)\right). \tag{81}$$

The corresponding value of ν is denoted by ν_0, and equal to $\alpha - \Omega_0$. It satisfies the following features: for $\nu > \nu_0$, q is negative, while for $\nu < \nu_0$, q is positive.

B.4. Absolute value of the q coefficient

The expression of q reads

$$q = \frac{-\delta|2\Omega + 1|(\alpha^2 + 4\Omega^2(\Omega + 1) + \alpha\Omega(3 + 4\Omega))}{2(1 + \alpha)|\Omega||(4\alpha + 1)\Omega + 3\alpha|} \tag{82}$$

where q diverges for two values of Ω; the first one is $\Omega = 0$, corresponding to $\nu = \alpha$: it is the asymptotic value of the frequency on the acoustic branch. The other value of Ω for which $|q|$ tends to infinity does not correspond to a physical wave (it yields $\delta = -1$ and $\alpha < \nu < 1 + \alpha$). Thus q shows no singularity for any frequency.

For waves with negative helicity ($\delta = +1$), q is negative and its absolute value grows monotonically from $q = \frac{-(2\alpha+1)}{\alpha+1}$, near the point $(k, \omega) = (0, 0)$, to infinity for large values of ν. It has the following asymptotic expression:

$$q = \frac{-4\nu^2}{(1 + \alpha)(1 + 4\alpha)} + \mathrm{O}(\nu). \tag{83}$$

For waves with positive helicity ($\delta = -1$) from the acoustic branch, q is always positive. It decreases from the value $q = \frac{(2\alpha+1)}{\alpha+1}$ at $\nu = 0$, to some minimal value, and then increases to infinity when ν tends to α, as mentioned above, with the asymptotic expression

$$q \simeq \frac{\alpha}{6(1 + \alpha)(\alpha - \nu)} + \frac{4 + \alpha}{9(1 + \alpha)} + \mathrm{O}(\alpha - \nu). \tag{84}$$

Despite the fact that an explicit expression of the minimum can be written, it is too complicated in practice. For large values of α, this minimum is located at about $\nu \simeq \alpha - \sqrt{\alpha}/2$. As $\nu = \alpha \mp \sqrt{\alpha}/2$, q has expression (32). It gives a good order of magnitude of the minimal value of q for α large enough, say $\alpha \geqslant 10$.

The behaviour of q on the third branch, optical with positive helicity, is not so simple. q cancels for the above-mentioned value ν_0 of ν, and then decreases to $-\infty$, with the same asymptotic expression (83) as the expression of q in the case of the wave with negative helicity. When ν varies from the singularity of q to ν_0, q passes through a minimum and then through a maximum. For large values of α, the minimum occurs at $\nu \simeq \alpha + \sqrt{\alpha}/2$, and the maximum at $\nu \simeq 3\alpha/2$. An approximate value of the minimum is given by (32), while the maximum is given by the value of q when $\nu = 3\alpha/2$:

$$q = \frac{\alpha - 1}{4\alpha - 5}. \tag{85}$$

For small values of α both the minimum and the maximum are smaller than $1 + \alpha$ and therefore do not belong to the set of the values that have a physical meaning. Clearly, $3\alpha/2$ is smaller than $\alpha + 1$ as soon as $\alpha < 2$. It is not worth computing a more accurate limiting value because the values of q at the maximum and minimum are very close together, for all values of α from about 1 to 8. The value taken at $\nu = \alpha + 1$ is a local maximum, and reads as $q = \frac{\alpha}{2(1+\alpha)}$.

B.5. Study of the r coefficient

According to expressions (71), (72), and especially (74), and using the result $\epsilon_2 = -\delta$, expression (22) of r reduces to

$$r = \frac{\delta}{\Omega + 1}. \tag{86}$$

The variations of r follow directly: for negative helicity, r is positive and decreases from $1/(1+\alpha)$ when $\nu = 0$, to zero as ν tends to infinity. For positive helicity, on the acoustic branch, r is also decreasing, but negative, varying from $-1/(1+\alpha)$ when $\nu = 0$, to -1 as ν tends to α. On the optical branch, r is positive, decreasing from $+\infty$ as ν tends to $1+\alpha$ and to 0 as ν tends to infinity.

References

[1] Davey A and Stewartson K 1974 On 3D packets of surface waves *Proc. R. Soc.* A **338** 101

[2] Satsuma J and Ablowitz M J 1979 Two-dimensional lumps in nonlinear dispersive systems *J. Math. Phys.* **20** 1496

[3] Boiti M, Leon J J-P, Martina L and Pempinelli F 1988 Integrable nonlinear evolutions in 2 + 1 dimensions with non-analytic dispersion relations *J. Phys. A: Math. Gen.* **21** 3611

[4] Boiti M, Leon J J-P, Martina L and Pempinelli F 1988 Scattering of localized solitons in the plane *Phys. Lett.* A **139** 432

[5] Boiti M, Leon J J-P and Pempinelli F 1990 Multidimensional solitons and their spectral transforms *J. Math. Phys.* **31** 2612

[6] Hietarinta J and Hirota R 1990 Multidromion solutions to the Davey–Stewartson equation *Phys. Lett.* A **145** 237

[7] Colin T Rigorous derivation of the nonlinear Schrödinger equation and Davey–Stewartson systems from quadratic hyperbolic systems *Preprint*

[8] Leblond H 1998 Bidimensional solitons in a quadratic medium *J. Phys. A: Math. Gen.* **31** 5129–43

[9] Besse C and Bruneau C H 1998 Numerical study of elliptic–hyperbolic Davey–Stewartson system: dromions simulation and blow-up *Math. Models Methods Appl. Sci.* **8** 1363

[10] Kalinikos B A and Slavin A N 1986 Theory of dipole-exchange spin wave spectrum for ferromagnetic films with mixed exchange boundary conditions *J. Phys. C: Solid State Phys.* **19** 7013

[11] Cottam M G (ed) 1994 *Linear and Nonlinear Spin Waves in Magnetic Films and Superlattices* (Singapore: World Scientific)

[12] De Gasperis P, Marcelli R and Miccoli G 1987 Magnetostatic soliton propagation at microwave frequency in magnetic garnet films *Phys. Rev. Lett.* **59** 481

[13] Kalinikos B A, Kovshikov N G and Slavin A N 1990 Experimental observation of magnetostatic wave envelope solitons in yttrium iron garnet thin films *Phys. Rev.* B **42** 8658

[14] Chen M, Tsankov M A, Nash J M and Patton C E 1993 Microwave magnetic-envelope dark-solitons in yttrium iron garnet thin films *Phys. Rev. Lett.* **70** 1707

[15] Büttner O, Bauer M, Demokritov S O, Hillebrands B, Kostylev M P, Kalinikos B A and Slavin A N 1999 Collisions of spin wave envelope solitons and self-focused spin-wavepackets in yttrium iron garnet films *Phys. Rev. Lett.* **82** 4320

[16] Bauer M, Büttner O, Demokritov S O, Hillebrands B, Grimalsky V, Rapoport Yu and Slavin A N 1998 Observation of spatiotemporal self-focusing of spin waves in magnetic films *Phys. Rev. Lett.* **81** 3769

[17] Leblond H and Manna M 1994 Focusing and defocusing of electromagnetic waves in a ferromagnet *J. Phys. A: Math. Gen.* **27** 3245–56

Leblond H and Manna M 1994 Benjamin–Feir type instability in a saturated ferrite. Transition between a focusing and defocusing regimen for polarized electromagnetic wave *Phys. Rev.* E **50** 2275–86

[18] Walker A D M and McKenzie J F 1985 Properties of electromagnetic waves in ferrites *Proc. R. Soc.* A **399** 217

[19] Hogan C L 1953 The ferromagnetic Faraday effect at microwave frequencies and its applications *Rev. Mod. Phys.* **25** 253

[20] Soohoo R F 1960 *Theory and Application of Ferrites* (London: Prentice-Hall)

[21] Bass F G and Nasonov N N 1990 Nonlinear electromagnetic-spin waves *Phys. Rep.* **189** 165

[22] Temiryazev A G 1989 Modulational instability of electromagnetic-spin waves in ferrite film *JETP Lett.* **50** 228

[23] Lecraw R C, Spencer E G and Porter C S 1958 Ferromagnetic resonance line width in yttrium iron garnet single crystals *Phys. Rev.* **110** 1311

[24] Leblond H 1996 Electromagnetic waves in ferrites: from linear absorption to the nonlinear Schrödinger equation *J. Phys. A: Math. Gen.* **29** 4623–39

[25] Kates R E and Kaup D J 1994 Two-dimensional nonlinear Schrödinger equations and their properties *Physica* D **75** 458

[26] Ghidaglia J M and Saut J C 1990 On the initial value problem fot the Davey–Stewartson systems *Nonlinearity* **3** 475

[27] Rasmussen J J and Rypdal K 1986 Blow-up of nonlinear Schroedinger equations I: a general review *Phys. Scr.* **33** 481
[28] Leblond H 1996 Phase boom for an electromagnetic wave in a ferromagnet *J. Phys. A: Math. Gen.* **29** 2805–25